Contents list available at IJRED website

Int. Journal of Renewable Energy Development (IJRED)

Journal homepage: https://ijred.undip.ac.id

Research Article

Mathematical Model of the Thermal Performance of Double-Pass Solar Collector for Solar Energy Application in Sierra Leone

Abu Bakarr Momodu Bangura[1]*, Ridho Hantoro[1], Ahmad Fudholi[2,3], Pierre Damien Uwitije[4]

[1]*Department of Engineering Physics, Institut Teknologi Sepuluh Nopember, Surabaya 60111, Indonesia*

[2]*Solar Energy Research Institute, Universiti Kebangsaan Malaysia, 43600 Bangi Selangor, Malaysia*

[3]*Research Centre for Electrical Power and Mechatronics, Indonesia Institute of Sciences (LIPI), Bandung, Indonesia*

[4]*Mechanical & Energy Engineering, University of Rwanda, Rwanda*

Abstract. The primary aim of this study was to utilize thermal energy for drying applications on March 21 (day of the year, n = 80) for the climatic weather conditions of Freetown, Sierra Leone. We evaluated the heat absorption of a double-pass solar air collector based on its configuration and exterior input variables before it was designed and mounted at the location of interest. This study considered a steady-state heat transfer using the thermal network procedure for thermodynamic modeling of a double-pass solar collector developed for drying and heating purposes. A mathematical model defining the thermophysical collector properties and many heat transfer coefficients is formed and numerically solved for this purpose. Indeed, this helped us generate the hourly temperature of different heat collector components, which aided in the performance evaluation of the system. The impact of the fluid flowing inside the collector on the temperature of the exit air was analyzed. It was observed that a flow rate of 0.02 kg/s produced an output of 91.72°C. The system's thermal efficiency improves with increased flow rate at various solar radiation intensities. It was observed that the thermal efficiency of the collector increases from 29% to 67% at flow rates of 0.01–0.3 kg/s. Collector lengths of 1.4 and 2.4 m are observed to be economically viable. An increase in the flow rate caused an increase on the efficiency. The hourly outputs for the collector components were represented graphically, and the curve patterns were similar to those of previous studies.

Keywords: Double-pass solar collector, Mathematical model, Mass flow rate, Thermal efficiency, Solar energy.

Article History: Received: 11th Sept 2021; Revised: 18th November 2021; Accepted: 10th December 2021; Available online: 2nd January 2022
How to Cite This Article: Bangura, A.B.M., Hantoro, R., Fudhloli, A., Uwitije, P.D.(2022) Mathematical Model of the Thermal Performance of Double-pass Solar Collector for Solar Energy Application in Sierra Leone. *Int. J. Renew. Energy Dev*, 11(2), 347-355
https://doi.org/10.14710/ijred.2022.41349

1. Introduction

The provision of heated air for product drying and some other heating purposes, particularly during unfavorable weather conditions, is one of the most significant goals for global solar energy utilization. Various solar air heating systems were already proposed and discussed. When comparing the benefits of these systems, the designer and future consumer must weigh various factors. The three key categories are (i) system efficiency, (ii) cost, and (iii) lifespan, reliability, upkeep, and flexibility of the system setup. The principle of thermal efficiency is used to compare the thermal output of collectors. It is widely assumed that a solar collector's thermal efficiency is the most crucial factor in predicting the solar system's thermal outcome. The solar air heater is a component (Chandra & Sodha, 1991; El-Sebaii *et al*., 2011).

Solar air heaters are the most popular since they are uncomplicated, inexpensive, and extensively utilized. Its primary applications are residential heating, solar dehydration, and manufacturing processing energy. The solar collector is typically the critical equipment in a thermal drying system. In tropical and temperate regions, solar drying technologies remain by far the most appealing and feasible deployments of solar energy systems (Fudholi *et al*., 2011). Solar drying technologies may evolve in various ways with respect to technological advancement. Solar drying systems must, first and foremost, be low-cost, low-power, and low-efficiency drying devices with a short lifespan. Secondly, solar collectors must exhibit excellent performance, high output, and a longer lifespan heating device (Ruslan et al., 2009).

Many analytical and practical studies have been conducted on several types of solar collector configurations (Tadesse, 2017). There are several design options for the

* Corresponding author: abangura781@yahoo.com

traditional single-pass solar collector. These technologies must be capable of reducing thermal dissipation from the collector, resulting in substantial system functioning temperatures and increased collector performance (Naphon, 2005). As a result, a single-pass solar air heater with heat exchange materials has been developed, using low-cost adsorbent materials such as granite, crumbled glass, metal chips, and sand (Ruslan *et al.,* 2013a). A multi-pass solar air collector with enhanced heat exchange enhancement characteristics such a V-corrugated collector and backup materials is superior to that of a single-pass solar collector with respect to efficacy (Fakoor Pakdaman *et al.,* 2011).

A solar collector converts solar radiation into heat energy, which is subsequently absorbed by a flowing fluid within the collector for a variety of purposes, including drying agricultural goods and device ventilation. Passive solar air collectors are the primary component in different solar drying systems for crop and marine goods (Sopian *et al.,* 2010). The solar collector's simultaneous performance fluctuates depending on the design, sunny days, and climate parameters. The ability to optimize the efficiency of a solar collector device is made possible by understanding its operational conditions. Several practical and theoretical studies have been conducted on solar collectors. Various practical and theoretical investigations on solar air heaters were already undertaken in various geographic regions to enhance their instantaneous efficiency (Bennamoun & Belhamri, 2011).

Due to their designs, conventional solar air collectors have low thermal performance. Utilizing an expanded heat transfer area, such as corrugated surfaces, is one way to significantly increase collector efficiency (Fudholi et al., 2008), porous media (Sopian *et al.*, 1999), and finned absorbers. Fudholi *et al.* (2008) reported that a corrugated solar collector is 7.4% quite effective than other types of solar heaters at a volume flow rate of 6.8 m3/s, according to their findings. Sopian *et al.* (1999) revealed that the average thermal effectiveness of a double-pass solar collector with a backup system is calculated to be above 60%. According to Ruslan *et al.* (2010b), at flow rates of 0.04-0.08 kg/s and solar intensities of 420–790 W/m^2, finned absorbers are 2%–8% quite effective over smooth surface absorbers. Ali Alfegi *et al.* (2009) concluded that by incorporating fins into the absorber's exterior, significant heat and electrical yield efficiencies of the combined PV/T solar collector can be achieved. Choudhury *et al.* (1995) examined the cost-effective design of a counter flow solar collector with a backup system unit for solar energy storage. Choudhury *et al.* (1995) revealed that double-pass solar collectors are efficiently and economically viable. The theoretical design of triple pass solar collectors with single and double glazing was investigated by Choudhury *et al.* (1996). Single-pass solar collectors without glazing, single and double glazing, and double-pass solar collector with single and double glazing were contrasted to the effectiveness of these solar collectors. The findings were displayed as a series of design curves.

A theoretical analysis of a double-pass solar collector is proposed in this study to predict the system's performance under Freetown's climatic weather conditions. The primary goal was to conduct a mathematical formulation of the system's heat exchange characteristics. The influence of various related parameters on the system's heat transfer characteristics was also examined.

2. Methods

The temperature of the boundaries governing the air flow is consistent in a small collector. According to the theoretical model, the airflow temperature differs uniformly from the collector. The wall and average air temperatures in the first segment are previously assumed and defined. The heat exchange parameters are determined based on the temperature values that were initially estimated. Excel was employed to compute the average temperature vector by inverting the function matrix (Sopian *et al*., 2013):

$$[T] = [X]^{-1}[Y]. \tag{1}$$

As such, the conceptual model suggests that the temperatures of the wall governing the air movement are constant for a small solar air heater (smaller than 10 m). As such, the air stream temperature differs uniformly along with the collector. The average air temperature for the short collector will be the same as the arithmetic average reported by Ruslan *et al.* (2013).

$$T_{f1} = (T_{f1,o} + T_i)/2 \tag{2}$$

$$T_{f2} = (T_{f2,o} + T_{f1,0})/2 \tag{3}$$

The following are the key concept parameters: $L = 240\ cm, W = 120\ cm, U_b = 1.0\ W/m^2°C$, $k_{ap} = 211.0\ W/m\ °C$, $T_a = T_i = 23\ °C$, and $V_w = 1.0\ m/s$ (Sopian et al., 2013). Normally, the initial conditions for a double-pass solar collector are at $x = 0$ and $T_{f1,i} = T_a$ for the first airflow stream and at $x = L$ and $T_{f2,i} = T_{f1,o}$ for the second airflow stream.
The solar collector's thermal efficiency is determined by Ong (1995) and Sopian *et al*. (2013).

$$\eta = \frac{\dot{m}C(T_o - T_i)}{A_c I} \tag{4}$$

The concept of a double-pass solar collector is shown in Fig. 1(a). The steady-state energy balance in this counter flow segment is investigated using the thermal network depicted in Fig. 1(b).

The steady-state heat transfer equations for the double-pass solar collector components considered as a node in the thermal network are as follows:

Exchange on the surface of the glass cover:

$$P_g + hr_{ap,g}(T_{ap} - T_g) + hc_{g,f1}(T_{f1} - T_g) = U_t(T_g - T_a) \tag{5}$$

Exchange on the first airflow stream:

$$hc_{ap,f1}(T_{ap} - T_{f1}) = Q_{u1} + hc_{g,f1}(T_{f1} - T_g) \tag{6}$$

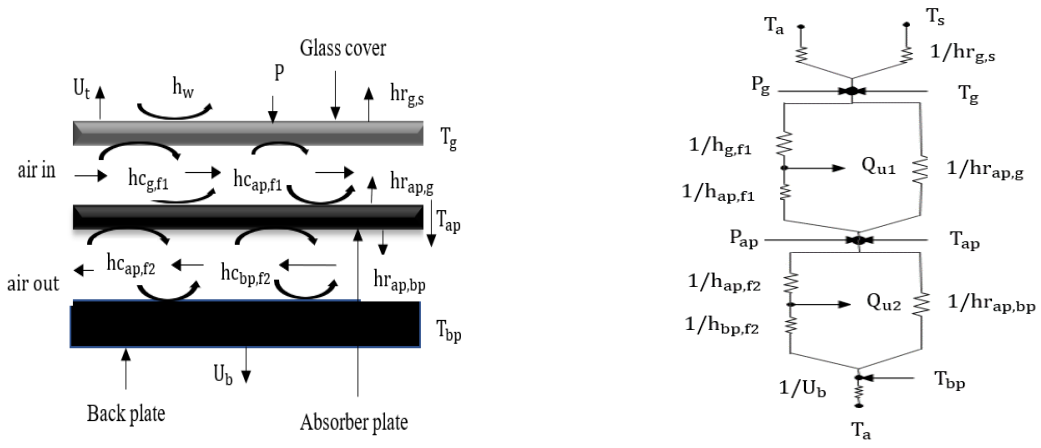

(a) **(b)**

Fig. 1. (a) Layout of double-pass solar collector. (b) Layout of thermal network for double-pass solar collector.

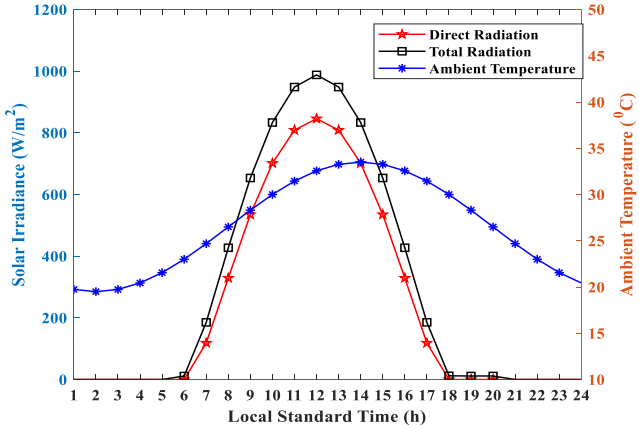

Fig. 2. Evolution of the hourly ambient temperature and solar radiation absorbed by a solar collector on March 21.

Exchange at the absorber plate surface:

$$P_{ap} = hc_{ap,f1}(T_{ap} - T_{f1}) + hr_{ap,g}(T_{ap} - T_g) + hc_{ap,f2}(T_{ap} - T_{f2}) + hr_{ap,bp}(T_{ap} - T_{bp}) \quad (7)$$

Exchange on the second airflow stream:

$$hc_{ap,f2}(T_{ap} - T_{f2}) = hc_{f2,bp}(T_{f2} - T_{bp}) + Q_{u2} \quad (8)$$

And lastly, exchange at the backplate surface:

$$hr_{ap,bp}(T_{ap} - T_{bp}) + hc_{f2,bp}(T_{f2} - T_{bp}) = U_b(T_{bp} - T_a). \quad (9)$$

To solve the obtained equations [Eqs. (5)–(9)], we applied the matrix inversion technique employing Excel, using which we calculated all the heat transfer coefficients (HTCs). HTCs are rated based on the temperature values that were initially assumed. The matrices [X], [T], and [Y] are then established, wherein the vector [T] denotes the vector of the five unknown parameters of the solar collector's five components. The temperature matrix $[X]^{-1}$ was then inverted using a regular matrix inversion subroutine to produce a new collection of temperature matrix [X′]. The corresponding previously estimated [T] is being compared to each current temperature value in the matrix [X′]. The iteration was ended when the variance between these corresponding old and new values reached 0.01 °C. The old temperatures were substituted with the recently measured ones and recorded as the needed temperatures in the interest area. The next time step was calculated. In most cases, four to six iterations are required to achieve adequate convergence of the collector component temperatures (Ong, 1995; Sopian *et al.*, 2013).

2.1. Input Parameters

As input parameters, the radiation gradient and ambient temperature played a significant part. In this analysis, we intend to compute such parameters theoretically. Fig. 2 illustrates the measurement of reflected, direct, and diffused radiation to calculate the total energy captured by the absorber and glass cover.

The analytical formulation has been developed for Freetown (latitude 8.484° N, longitude −13.230° W at an

elevation of 26 m from mean sea level). Input operational parameters employed for analytical calculations are given as: $\beta = 15^{\circ}$, $T_i = T_a = 23°C$, $\varepsilon_g = 0.8$, $\varepsilon_{ap} = 0.9$, $\tau_g = 0.92$, $\alpha_g = 0.05$, $\alpha_{ap} = 0.95$, $\gamma = 0.2$, and $\sigma = 5.67 \times 10^{-8}$ $Wm^{-2}K^{-4}$.

Several formulas involved in estimating prominent solar angles were used to determine the overall input parameters using the ASHRAE model for sunny weather (Goswami, 2015). This ASHRAE mathematical model is defined for Freetown weather conditions on March 21 (day of the year, n = 80). March 21 was selected in accordance with the ASHRAE model. Based on the meteorological weather conditions of Freetown, March is the clearest and cloudless month among the other months of the year. In essence, the model works well in predicting the collector output temperatures during the month under review. Due to Sierra Leone's temperate climate, the ambient temperature data were calculated using the sinusoidal formula, with mean peak and lowest temperatures of 30°C and 23°C, respectively, for March (Goswami, 2015). The predicted results are depicted in the blue curve in Fig. 2.

2.2. Heat Transfer Coefficient Estimation

In a solar collector component, there are essentially three main thermal transfer processes. The physical characteristics of air are thought to change uniformly as the temperature rises (Ong, 1995):
Air's specific heat capacity (Ali Alfegi et al., 2009):

$$Cp = 1.0057 + 0.000066(T - 27) \quad (10)$$

Air density (Ong, 1995):

$$\rho_{air} = 1.1774 - 0.00359(T - 27) \quad (11)$$

Thermal conductivity of air (Ali Alfegi et al., 2009):

$$k = 0.02624 + 0.0000758(T - 27) \quad (12)$$

Viscosity of air (Ong, 1995):

$$\mu_{air} = [1.983 + 0.00184(T - 27)] * 10^{-5} \quad (13)$$

with

$$T = (T_{f1} + T_g)/2. \quad (14)$$

The coefficients of thermal exchange for various modes are determined as follows (Timoumi *et al.*, 2004; Pascal *et al.*, 2017):

Convective HTC due to wind:

$$h_w = 2.8 + 3.3V \quad (15)$$

Exchange across the glass surface and sky by radiation:

$$hr_{g,s} = \frac{\sigma\varepsilon_g(T_g + T_s)(T_g^2 + T_s^2)(T_g - T_s)}{(T_g - T_a)} \quad (16)$$

with $T_s = 0.0552.T_a^{1.5}$

Exchange across the glass cover and absorber plate by radiation:

$$hr_{ap,g} = \frac{\sigma\varepsilon_{ap}\varepsilon_g(T_{ap} + T_g)(T_{ap}^2 + T_g^2)}{\varepsilon_{ap} + \varepsilon_g - \varepsilon_{ap}\varepsilon_g} \quad (17)$$

Exchange across the absorber plate and backplate by radiation:

$$hr_{ap,bp} = \frac{\sigma\varepsilon_{ap}\varepsilon_{bp}(T_{ap}+T_{bp})(T_{ap}^2+T_{bp}^2)}{\varepsilon_{ap}+\varepsilon_{bp}-\varepsilon_{ap}\varepsilon_{bp}}. \quad (18)$$

The convective heat exchange through the absorber and back surfaces with the fluid movement in this stream are calculated using the following equation (Ong, 1995):

$$hc = \frac{k}{D_h} Nu \quad (19)$$

$$Nu = 0.036.Re^{0.8}.Pr^{(1/3)}(D_h/L) \quad (20)$$

$$Re = (V.D_h.\rho_{air})/\mu_{air} \quad (21)$$

$$D_h = \frac{4.W.d}{2.(W + d)} \quad (22)$$

$$V = \dot{m}/(\rho_{air}.W.depth). \quad (23)$$

3. Result and Discussion

The climate parameters directly impact the operation of a solar energy collector. The solar radiation data and predicted atmospheric temperatures for Sierra Leone are graphically illustrated. It should be noted that atmospheric temperatures are determined by the intensity of solar radiation striking the Earth, which explains the lower ambient temperatures found at night because there would be less irradiance. On the other hand, the peak total solar radiation value occurs at 12 noon. In contrast, the peak ambient temperature value lags the peak solar radiation by 3 h and lies between 13:00 and 15:00 pm, as shown in the blue curve of Fig. 2. According to Jain and Jain (2004), the peak ambient temperature occurs between 15:00 and 16:00 pm, which is 2 h delayed the optimum solar radiation.

The theoretical findings for the designed double-pass solar collector are displayed in Fig. 3. The system performance was low in the morning and high in the afternoon. The system delivered fluid exit temperatures above 50°C from 8:00 am until 16:00 pm, at a flow rate of 0.02 kg/s, with a peak fluid exit temperature of 96°C generated at midday. Pascal *et al.* (2017) investigated the experimental characteristics of a single-pass flat surface solar collector and reported a fluid temperature output of approximately 60 °C. Karim *et al.* (2014) reported a fluid exit temperature of approximately 307.32 K at $m = 0.035\ kg/m^2s$ when investigating the analytical modeling of a double-pass corrugated solar collector. Jain (2007) reported the fluid output temperature of the reversed absorber with packed bed to be approximately 80 °C.

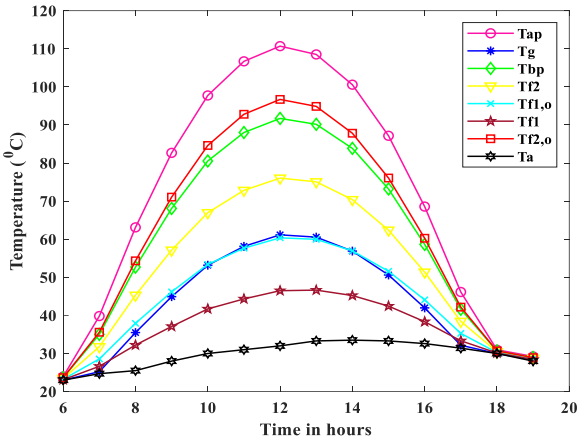

Fig. 3. Hourly variation of fluid and solar collector component temperatures at different phases of the collector for $L = 240\,cm, b = 120\,cm, \beta = 15^0$, and $\dot{m} = 0.02$ kg/s.

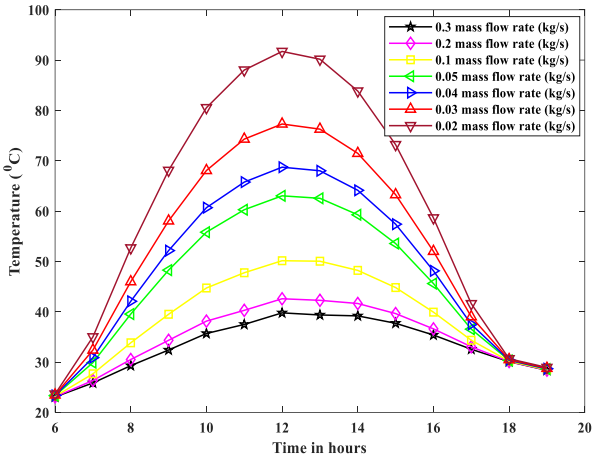

Fig. 4. Variation of fluid mass flow rate inside the solar collector of the fluid exit temperatures.

Fig. 4 depicts the effect of varying the mass flow rate of the fluid moving within the solar collector. The mass flow rate is, without a doubt, a critical variable in every solar collector system. The flow rate moving at 0.02 kg/s could be heated up to 91.72°C, the flow rate moving at 0.03 kg/s can reach up to 77.3°C, that at 0.04 kg/s was observed to be 68.72°C, the flow rate at 0.05 kg/s can only achieve 63°C, and the flow rates flowing at 0.1, 0.2, and 0.3 kg/s can be heated up to 50.14°C, 42.58°C, and 39.78°C, respectively. Such findings are attributed to the reality that the relatively slow the air flows, the longer it takes to warm up the collector. This influence of air movement ability appears to be a significant factor. This is evidenced by the fact that the airflow gap at 0.02 kg/s is more critical than that at 0.3 kg/s. Aldabbagh *et al.* (2010) reported fluid exit temperatures of approximately 27°C and 38.8 °C at 13:00 pm for single and double-pass solar collectors, respectively, at a flow rate of 0.012 kg/s using a wire mesh. Fig. 5 displays the variation of the fluid exit temperatures of various segments of the collector for flow rates ranging from 0.01 to 0.1 kg/s at 988 W/m² solar radiation. The curve trends showed that an increase in flow rate led to a decrease on the fluid exit temperatures of various components of the collector. It was noted that the fluid exit temperatures are strongly dependent on the flow rate. At a flow rate of 0.01 kg/s, the optimal fluid exit temperature was observed to be 111.43°C. According to Sopian *et al.* (2013), an increase in the flow rates instantaneously lowered the fluid exit temperatures of various segments of the double-pass solar collector with and without fins at certain solar radiation values.

Fig. 6 depicts the influence of flow rate on the thermal efficiency of the collector for various solar radiation intensities. A thermal efficiency of approximately 29%–67% of the collector was observed at flow rates of 0.01–0.3 kg/s. At a flow rate of 0.3 kg/s and at a solar radiation value of 948 W/m², the collector's efficiency was approximately 67%. The efficiency was observed to increase by 38% at flow rates of 0.01–0.3 kg/s and at solar radiations varying from 185 to 948 W/m². Consequently, as depicted on the curve trends of Fig. 6, an increase in flow rate led to a corresponding increase in the thermal efficiency of the system. It was observed that the flow rate strongly influences the system's thermal efficiency. Ruslan *et al.* (2010a) reported an efficiency increase of approximately 40% at flow rates of 0.04–0.08 kg/s by employing a double-pass solar collector with fins, at a varied solar radiation of 423–788 W/m².

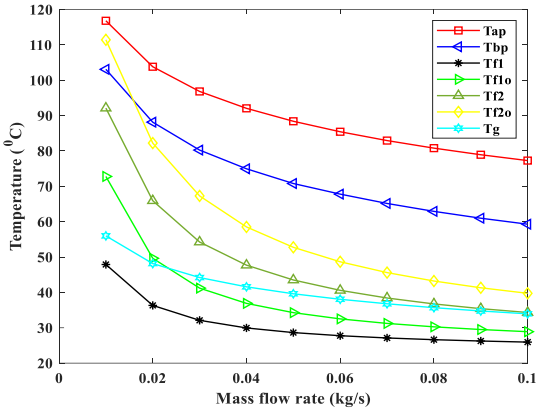

Fig. 5. Variation of fluid exit temperatures as a function of mass flow rate at 988 W/m^2 irradiance.

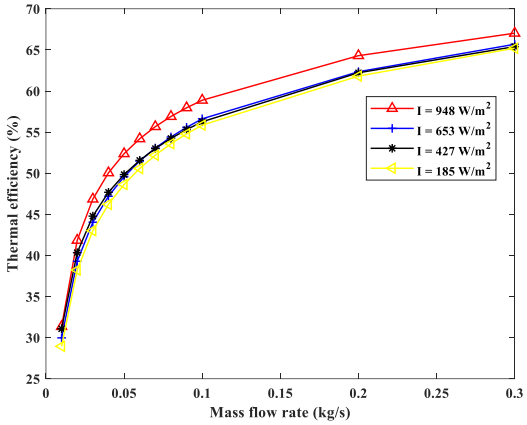

Fig. 6. Influence of mass flow rate on the solar collector's thermal efficiency at varying solar radiation intensities.

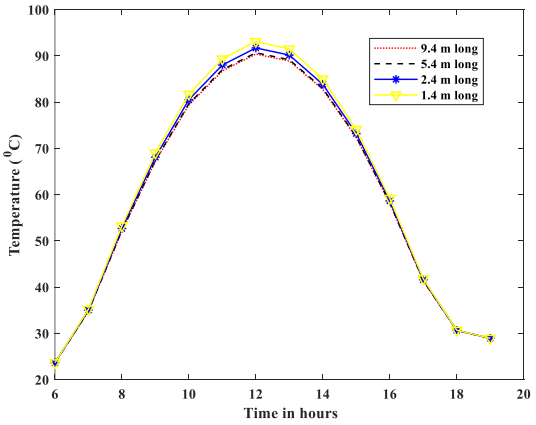

Fig. 7. Influence of collector length as a function of time on the outlet air temperatures.

The solar collector's performance is essentially influenced by the amount of solar radiation it absorbs. The longer the collector length, the most solar energy is transformed to heat. Nonetheless, depending on the temperature required, the length of the collector must be tailored for cost effectiveness and practicality. Fig. 7 illustrates the fluid outlet temperatures as a function of time for different solar collector lengths. It is generally thought that the greater the collector surface, the prolonged time it takes to warm up. In the present study, varying the collector surface does not influence the fluid outlet temperatures that much. The observed temperatures from the four collector surfaces investigated are nearly similar. The features of a double-pass solar collector provide an interpretation of this observation. Apparently, the optimal temperature outputs for collector

surfaces of 1.4, 2.4, 5.4, and 9.4 m are 93.10 °C, 91.72 °C, 90.67°C, and 90.39°C, respectively, which were all observed at 12:00 pm. In the present study, the collector lengths of 1.4 and 2.4 m are critical and can be optimized for economic purposes. However, in this investigation, a flow rate of 0.02 kg/s was used. Bala and Woods (1994) investigated three collector lengths of 2, 3, and 4 m, and their findings showed that a collector length of 2 m produced a fluid exit temperature of approximately 60 °C To evaluate the collector's physical characteristics, we can represent the effectiveness with the efficiency lines, as illustrated in Fig. 8. As seen in Fig. 8, as the reduce temperature variables increase, the efficiency declines exponentially. In essence, the efficiency is highly dependent on the reduced temperature parameters. The graph shows a plain pattern, with intercept on the ordinate axis equals Fo (τα) and gradient equals FoU_L, where Fo is the heat reduction variable termed as fluid outlet temperature of the system, U_L is the system loss index, τ is the transmissivity, and α is the absorptivity of the system. Table 1 shows different efficiency notations as well as system conceptual features. Ruslan et al. (2010a) reported a coefficient of determination (R^2) values of 0.97, 0.92, and 0.98 for solar radiation values of 788, 572, and 423 W/m², respectively.

4. Conclusion

A double-pass solar collector was theoretically analyzed to determine its thermal performance using a mathematical model solution approach. Conversely, a matrix inversion approach was employed. The system was examined using thermal heat transfer equations, which were developed to periodically determine the outlet air temperature for various collector elements. It must be recognized that solar radiation and ambient temperature are the two key variables affecting the fluid exit temperatures. The intensity of solar radiation influences the ambient temperature during the day. The system performance in the morning hours was low because there were fewer solar radiation and ambient temperature at this period. Between 8:00 am and 16:00 pm, the system started to generate higher temperatures. It was evidenced that the mass flow rate had a corresponding influence on the fluid outlet temperatures. It was also observed that the influence of the flow rate of the fluid moving inside the collector on the temperature output. It was noted that the faster the fluid flows inside the collector, the faster the collector can be heated up. Fluid flowing at 0.02 kg/s was observed to be more crucial than that at 0.3 kg/s. The system's thermal performance is largely influenced by the fluid flow rate. The thermal efficiency of the system increased exponentially when the flow rate was increased. The system's optimal efficiency was observed to be 67% at a flow rate of 0.3 kg/s. An efficiency increase of 38% was noticed at flow rates of 0.01–0.3 kg/s and at solar radiation varying from 185–948 W/m². The improvement in efficiency increases in proportion to the magnitude of solar radiation intensity absorbed by the collector. The impact of the surface of the solar collector as a function of time was discussed. It was noted that the collector surfaces of 1.4 and 2.4 m are economically viable.

Table 1
Efficiency reduction variables and performance equations for the collector system

I (Wm^{-2})	F_0 (τα)	F_0U_L	Efficiency equations	R^2
185	0.67	2.3	Y = −378.32x + 59.623	0.9802
427	0.71	2.6	Y= −388.2x + 61.205	0.9833
653	0.74	2.9	Y = −406.85x + 64.494	0.9923

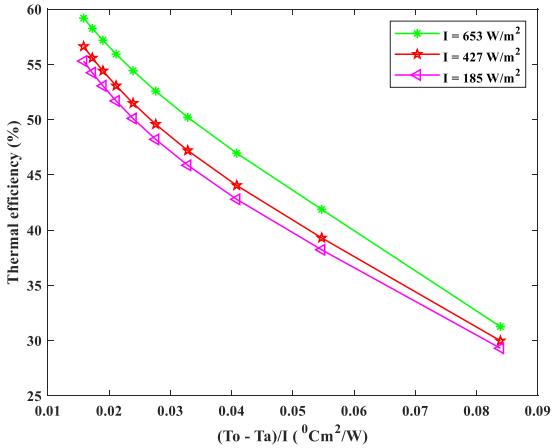

Fig. 8. Evolution of the collector's thermal efficiency as a function of the reduced temperature parameters $[(T_o - T_a)/I]$.

It was also observed the influence of the reduced temperature parameters on the collector's thermal efficiency. It was revealed that as the reduced temperature parameters increase, there is a gradual reduction on the thermal efficiency of the system. The studied system produced significant fluid temperature outputs for various parameters discussed, allowing it to be utilized for diverse heating and drying applications.

Numenclature

Ac	:	frontal area of solar collector (m^2)
Cp	:	specific heat capacity for working fluid (J/kg K)
Dh	:	equivalence diameter (m)
d	:	stream depth (m)
HTC	:	heat transfer coefficient (W/m^2 ^oC)
hc	:	heat transfer coefficient by convection (W/m2 °C)
hr	:	heat transfer coefficient by radiation (W/m^2 °C)
I	:	solar irradiation intensity (W/m^2)
k	:	thermal Conductivity (W/m^2 °C)
L	:	length of collector (m)
m	:	mass flow rate (kg/s)
Nu	:	Nusselt number (-)
P	:	Power absorbed (W/m^2)
Pr	:	Prandtl number (-)
Qu	:	heat transferred to air (W/m^2)
Re	:	Reynold number (-)
T	:	temperature (^oC)
Ub	:	bottom heat loss (W/m^2 °C)
Ut	:	top heat loss (W/m^2 °C)
Vw	:	wind velocity (m/s)
W	:	width collector (m)
η	:	efficiency (%)

Subscript

1&2	:	represent first and second streams
a	:	ambient temperature
ab	:	absorber plate
bp	:	backplate
f	:	fluid
g	:	glass cover
i	:	inlet
o	:	outlet
p	:	plate
s	:	sky
w	:	wind

Greek symbols

α	:	absorptivity
β	:	collector tilt angle
ε	:	emissivity
τ	:	transmissivity
σ	:	Stefan–Boltzmann constant ($Wm^{-2}K^{-4}$)
ρ	:	density (kg/m^3)
μ	:	viscosity (Pa s)
γ	:	reflectivity

References

Aldabbagh, L. B. Y., Egelioglu, F., & Ilkan, M. (2010). Single and double pass solar air heaters with wire mesh as packing bed. *Energy*, *35*(9), 3783–3787. https://doi.org/10.1016/j.energy.2010.05.028

Ali Alfegi, E. M., Sopian, K., Othman, M. Y. H., & Yatim, B. Bin. (2009). Mathematical model of double pass photovoltaic thermal air collector with fins. *American Journal of Environmental Sciences*, *5*(5), 592–598. https://doi.org/10.3844/ajessp.2009.592.598

Bala, B. K., & Woods, J. L. (1994). Simulation of the indirect natural convection solar drying of rough rice. *Solar Energy*, *53*(3), 259–266. https://doi.org/10.1016/0038-092X(94)90632-7

Bennamoun, L., & Belhamri, A. (2011). Study of solar thermal energy in the north region of Algeria with simulation and modeling of an indirect convective solar drying system. *Nature &Technology*, *4*(December 2013), 34–40.

Chandra, R., & Sodha, M. S. (1991). Testing procedures for solar air heaters: A review. *Energy Conversion and Management*, *32*(1), 11–33. https://doi.org/10.1016/0196-8904(91)90139-A

Choudhury, C., Chauhan, P. M., & Garg, H. P. (1995). Performance and cost analysis of two-pass solar air heaters. *Heat Recovery Systems and CHP*, *15*(8), 755–773. https://doi.org/10.1016/0890-4332(95)00003-H

Choudhury, C., Chauhan, P. M., Garg, H. P., & Garg, S. N. (1996). Cost-benefit ratio of triple pass solar air heaters. *Energy Conversion and Management*, *37*(1), 95–116. https://doi.org/10.1016/0196-8904(95)00017-8

El-Sebaii, A. A., Aboul-Enein, S., Ramadan, M. R. I., Shalaby, S. M., & Moharram, B. M. (2011). Investigation of thermal performance of-double pass-flat and v-corrugated plate solar air heaters. *Energy*, *36*(2), 1076–1086. https://doi.org/10.1016/j.energy.2010.11.042

Fakoor Pakdaman, M., Lashkari, A., Basirat Tabrizi, H., & Hosseini, R. (2011). Performance evaluation of a natural-convection solar air-heater with a rectangular-finned absorber plate. *Energy Conversion and Management*, *52*(2), 1215–1225. https://doi.org/10.1016/j.enconman.2010.09.017

Fudholi, A., Ruslan, M. H., Othman, M. Y., Yahya, M., Supranto, Zaharim, A., & Sopian, K. (2010a). Collector efficiency of the double-pass solar air collectors with fins. *International Conference on System Science and Simulation in Engineering - Proceedings*, 428–434.

Fudholi, A., Ruslan, M. H., Othman, M. Y., Yahya, M., Supranto, Zaharim, A., & Sopian, K. (2010b). Experimental study of the double-pass solar air collector with staggered fins. *International Conference on System Science and Simulation in Engineering - Proceedings*, *January*, 410–414.

Fudholi, A., Sopian, K., Ruslan, M. H., Alghoul, M. A., & Sulaiman, M. Y. (2010). Review of solar dryers for agricultural and marine products. *Renewable and Sustainable Energy Reviews*, *14*(1), 1–30. https://doi.org/10.1016/j.rser.2009.07.032

Fudholi, A, Sopian, K., Othman, M. Y., Ruslan, M. H., & Alghoul, M. A. (2008). Heat Transfer Correlation for the V-Groove Solar Collector. *8th WSEAS International Conference on Simulation, Modelling and Optimization (SMO '08) Santander, Cantabria, Spain, September 23-25, 2008 Heat*, *October 2014*, 177–182.

Fudholi, Ahmad, Ruslan, M. H., & Othman, M. Y. (2013a). Mathematical Model of Double-Pass Solar Air Collector. *Latest Trends in Renewable Energy and Environmental Informatics. Proceedings of the 7th International Conference of Renewable Energy Sources*, *May 2017*, 279–283.

Fudholi, Ahmad, Ruslan, M. H., & Othman, M. Y. (2013b). Mathematical Model of Double-Pass Solar Air Collector. *Latest Trends in Renewable Energy and Environmental Informatics. Proceedings of the 7th International Conference of Renewable Energy Sources*, 279–283.

Fudholi, Ahmad, Sopian, K., Ruslan, M. H., & Othman, M. Y. (2013). Performance and cost benefits analysis of double-pass solar collector with and without fins. *Energy Conversion and Management*, *76*, 8–19. https://doi.org/10.1016/j.enconman.2013.07.015

Fudholi, Ahmad, Sopian, K., Ruslan, M. H., Othman, M. Y., Yahya, M., Bangi, U. K. M., & Ehsan, S. D. (2011).

Analytical and Experimental Studies on the Thermal Efficiency of the Double-Pass Solar Air Collector with Finned Absorber Solar Energy Research Institute, University Kebangsaan Malaysia,. *American Journal of Applied Sciences*, *8*(7), 716–723.

Goswami, D. Y. (2015). Principles of Solar Engineering. In *Taylor & Francis Group*. https://doi.org/10.1115/1.1288930

Jain, D. (2007). Modeling the performance of the reversed absorber with packed bed thermal storage natural convection solar crop dryer. *Journal of Food Engineering*, *78*(2), 637–647. https://doi.org/10.1016/j.jfoodeng.2005.10.035

Jain, D., & Jain, R. K. (2004). Performance evaluation of an inclined multi-pass solar air heater with in-built thermal storage on deep-bed drying application. *Journal of Food Engineering*, *65*(4), 497–509. https://doi.org/10.1016/j.jfoodeng.2004.02.013

Karim, M. A., Perez, E., & Amin, Z. M. (2014). Mathematical modelling of counter flow v-grove solar air collector. *Renewable Energy*, *67*, 192–201. https://doi.org/10.1016/j.renene.2013.11.027

Naphon, P. (2005). On the performance and entropy generation of the double-pass solar air heater with longitudinal fins. *Renewable Energy*, *30*(9), 1345–1357. https://doi.org/10.1016/j.renene.2004.10.014

Ong, K. S. (1995). Thermal performance of solar air heaters: Mathematical model and solution procedure. *Solar Energy*, *55*(2), 93–109. https://doi.org/10.1016/0038-092X(95)00021-I

Pascal, P., Canissius, U., Germain, B., Alphonse, T., & Alidina, P. E. (2017). *Study and Modelisation the Parameters of Plate Solar air Collector at Single Pass for Drying of Madagascar CocoaBeans*. *8*, 8–14.

Ruslan, M. H., Fudholi, A., Othman, M. Y., Syahriman, M., Azmi, M., Yahya, M., Zaharim, A., & Sopian, K. (2009). The double-pass solar dryer for drying palm oil fronds. *Recent Researches in Power Systems and Systems Science*, 143–149.

Sopian, K., Supranto, Daud, W. R. W., Othman, M. Y., & Yatim, B. (1999). Thermal performance of the double-pass solar collector with and without porous media. *Renewable Energy*, *18*(4), 557–564. https://doi.org/10.1016/S0960-1481(99)00007-5

Tadesse, M. (2017). *Mathematical Modeling and Performance Analysis of V- Grooved single pass, V-Grooved Series and Parallel Flow Double Pass Solar Air Collectors*. *6*(7), 1–13.

Timoumi, S., Mihoubi, D., & Zagrouba, F. (2004). Simulation model for a solar drying process. *Desalination*, *168*(1–3), 111–115. https://doi.org/10.1016/j.desal.2004.06.175

This article was a selected paper from the 5th International Conference on Mechanical Engineering 2021 (ICOME 2021), 25th -26th August 2021, Surabaya